Vision-based Integrated Lateral Control System for Electric Vehicles Considering Multi-rate and Measurable Uneven Time Delay Issues

Yafei Wang
Department of Electrical Engineering,
Graduate School of Engineering,
The University of Tokyo, Tokyo, 113-0033, Japan
E-mail: wang@hori.k.u-tokyo.ac.jp

Binh Minh Nguyen, Hiroshi Fujimoto,
and Yoichi Hori
Department of Advanced Energy,
The University of Tokyo, Chiba, 227-8561, Japan
E-mail: minh@hori.k.u-tokyo.ac.jp,
fujimoto@k.u-tokyo.ac.jp, hori@k.u-tokyo.ac.jp

***Abstract*—Driver assistance systems such as automatic steering for lane keeping are of particular importance for vehicle's lateral safety, and onboard look-ahead cameras are widely employed to acquire surrounding information for realization of such applications. In fact, vision-based lane keeping and automatic steering have been intensively studied in the past few decades. Meanwhile, electric vehicles, as green solutions for future transportation, are gaining increasing attentions nowadays. From the viewpoint of motion control, differential torque between left and right in-wheel-motors is considered as an effective method for lateral safety control of electric vehicles. Nevertheless, the sampling rate of normal cameras is 30 Hz, which is much slower compared with that of motors and other kinds of onboard sensors. Moreover, image processing brings uneven time delay (which is usually measurable) into the visual signals, which further complicate the system sampling sequence. Many previous research simply adapt the whole system's sampling frequency to the camera; however, the held and random delayed feedbacks deteriorate system performance and may cause instability. In this paper, the two problems are solved by a multi-rate Kalman filter with random measurement delays compensation using a residual estimation technique.**

Keywords—Electric vehicle, integrated motion control, multi-rate estimation, measurable uneven measurement delay, vehicle lateral position, vision system.

I. INTRODUCTION

For vehicle safety control systems, online state information such as yaw rate and lateral position with reference to the road are considered as key enablers. In [1], a yaw moment control algorithm was developed using differential torque of in-wheel-motors (IWMs) for effective vehicle yaw motion stabilization. Another research tried to control both yaw rate and body slip angle at the same time using IWMs [2]. Yaw rate can be easily obtained from gyroscope which is widely used for a variety of motion control applications. On the other hand, automatic steering devices for lane keeping have been extensively investigated by automotive companies and research institutions. Joel C. McCall *et al.* surveyed some previous researches, proposed their own methods for lane detection and evaluated the methods with systematic criteria [3]. Another research was conducted by M. Bertozzi *et al*. [4], in which stereo vision system was employed to detect lane markers and obstacles on the road. While lane keeping strategies of these proposed methods differ somewhat, most of them use cameras and image processing systems for lane detection and location.

For yaw motion control and vehicle position control, most of the previous studies developed them independently [1]-[4]. However, they have to be considered together in many cases. For example, even if the yaw rate is controlled to be zero, the vehicle may deviate from the desired path [5]; on the other hand, the vehicle may spin even the vehicle is kept within the lane. That is, vehicle motion and position control should be considered in a systematic way. Therefore, some studies investigated integrated vehicle lateral stability systems such as control yaw rate and heading angle [5]. In this paper, an integrated lateral controller addressing yaw motion and vehicle position at the same time is investigated for electric vehicles (EVs). In fact, vehicle heading angle and vehicle lateral position are coupled as can be seen later in this paper, and they are equivalent in the sense of position control.

In case of EVs, the sampling time of traction motors is in millisecond-level. Considering the open loop stability margin, faster feedback is desirable compared with traditional vehicles using internal combustion engines and hydraulic actuator. Unfortunately, the sampling rate of normal cameras is not fast enough for realization of such motion control applications. That is, multi-rate issue exists in both state estimation and control for EVs. In addition, due to the variation of incoming images and processing loads, image processing time is not constant in practice. In this study, the information from vision system is considered to be random delayed. For measurement delay, a widely employed approach is to augment the states with delayed measurements. However, in case of uneven and large time delay as studied in this research, expansion of system state space equation is not practical. In this paper, the measurable uneven delay issue is solved with a residual reconstruction approach. Moreover, the aforementioned sampling mismatch of vision system and other onboard sensors is addressed in the Kalman filter design.

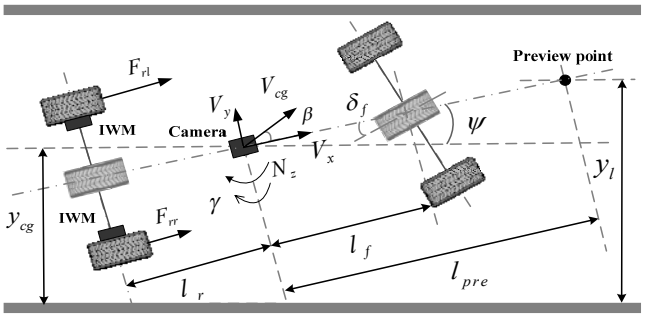

Fig. 1. Combined vehicle and vision model.

II. System Modelling

The model utilized in this research is constructed based on the model utilized in [6], and it is a combination of vehicle dynamic model and vision kinematic model. With this model, vehicle lateral position can be estimated accordingly.

For state estimation and control of EVs, bicycle model considering the yaw moment generated by the left and right IWMs is usually employed. The vehicle model used in this research is shown in Fig. 1, where F_{rl} and F_{rr} are the forces of IWMs, and they can be different for the generation of yaw moment N_z. The governing equations are given in equations (1) and (2), where β and γ are the body slip angle and the yaw rate at the vehicle's center of gravity (CoG), respectively, δ_f is the front-steering angle, V_x is the vehicle's longitudinal velocity, V_{cg} is the vehicle's velocity at CoG, m is the vehicle mass, I is the moment of inertia about the yaw axis, C_f and C_r are the cornering stiffness of the front and rear wheels, respectively, l_f and l_r are the distances from the CoG to the front and rear wheels, respectively.

$$m \cdot V_x \cdot (\dot{\beta} + \gamma) = 2 \cdot C_f \cdot (\delta_f - \frac{l_f}{V_x}\gamma - \beta) + 2 \cdot C_r \cdot (\frac{l_r}{V_x}\gamma - \beta) \quad (1)$$

$$I \cdot \dot{\gamma} = 2 \cdot l_f \cdot C_f \cdot (\delta_f - \frac{l_f}{V_x}\gamma - \beta) - 2 \cdot l_r \cdot C_r \cdot (\frac{l_r}{V_x}\gamma - \beta) + N_z \quad (2)$$

The vehicle dynamic model is independent of road reference, whereas the vision kinematic model is obtained from the geometric relationship between the vehicle and the road. The vision model is also shown in Fig. 1, where y_l is the lateral offset at a preview point, ψ denotes the heading angle, y_{cg} is the lateral offset at the vehicle's CoG, and l_{pre} is the fixed preview distance that needs to be calibrated beforehand. The gray borders in Fig. 1 are the lane makers, and the vision system is located at the vehicle's CoG. In this model, assumptions that the vehicle travels along a straight road and that the onboard vision system detects the lane and provides relative position information were made.

Vehicle lateral offset at a preview distance y_l and heading angle ψ can be described as equations (3) and (4). Detailed derivations can be found in [7].

$$\dot{y}_l = V_x \cdot \beta + l_{pre} \cdot \gamma + V_x \cdot \psi \quad (3)$$

$$\dot{\psi} = \gamma \quad (4)$$

Combining (1) to (4) yields a new system that is represented in a continuous state space form as equation (5). The first two states are modelled by the vehicle model and the latter two are modelled by the vision model. Clearly, the vision model contains much fewer uncertainties compared with the bicycle model.

$$\begin{aligned} \dot{x} &= A \cdot x + B \cdot u \\ y &= C \cdot x \end{aligned} \quad (5)$$

where

$$x = \begin{bmatrix} \beta & \gamma & \psi & y_l \end{bmatrix}^T, \quad u = \begin{bmatrix} \delta_f & N_z \end{bmatrix}^T, \quad y = \begin{bmatrix} \gamma & \psi & y_l \end{bmatrix}^T,$$

$$A = \begin{bmatrix} -\frac{2(C_f + C_r)}{m V_x} & -1 - \frac{2(C_f l_f - C_r l_r)}{m V_x^2} & 0 & 0 \\ -\frac{2(C_f l_f - C_r l_r)}{I} & -\frac{2(C_f l_f^2 + C_r l_r^2)}{I V_x} & 0 & 0 \\ 0 & 1 & 0 & 0 \\ V_x & l_{pre} & V_x & 0 \end{bmatrix},$$

$$B = \begin{bmatrix} \frac{2C_f}{m V_x} & \frac{2C_f l_f}{I} & 0 & 0 \\ 0 & \frac{1}{I} & 0 & 0 \end{bmatrix}^T, \quad C = \begin{bmatrix} 0 & 1 & 0 & 0 \\ 0 & 0 & 1 & 0 \\ 0 & 0 & 0 & 1 \end{bmatrix}.$$

In the combined vehicle and vision models, the measurable outputs are yaw rate, vehicle heading angle, and lateral offset at the preview point. The control inputs are steering angle and yaw moment.

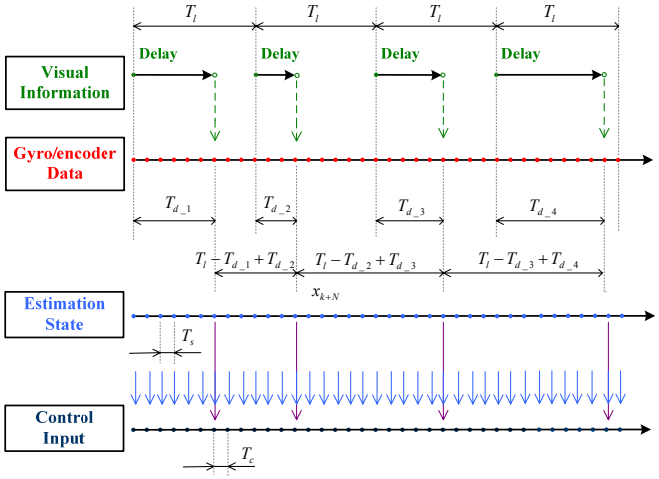

Fig. 2. Sampling sequence of sensing devices.

III. Problem Statement

To apply the Kalman filter in real time, equation (5) needs to be implemented in the discretized form, as shown in equation (6), where k is the time step. As the system model contains uncertainties and the sensor measurements are contaminated by noises, process noise w_k and measurement noise v_k are also included. The state space matrices are time varying because of changes in vehicle parameters.

$$\begin{aligned} x_{k+1} &= G_k \cdot x_k + H_k \cdot u_k + w_k \\ y_k &= C_k \cdot x_k + v_k \end{aligned} \tag{6}$$

where

$$G_k = e^{A \cdot T}, \quad H_k = \int_0^T e^{A \cdot \tau} \cdot B d\tau,$$

$$C_k = C, \quad T : sampling\ time$$

Unlike other kinds of onboard sensors, data from vision system is unevenly delayed and the sampling time of a camera is longer than the other sensors. The sampling sequence is shown in Fig. 2.

A. Uneven Sampled Visual Data

Measurements from the vision system are random delayed because of image processing. Therefore, the visual output equation becomes

$$y_k^{vis} = C \cdot x_{k-n_{d\_i}}^{vis} + v_{k-n_{d\_i}}^{vis} \tag{7}$$

where T_{d_i} is the time delay of the vision signals, i is the time visual stamp of image, and $i = 1, 2, 3, \ldots$, $n_{d\_i} = T_{d\_i} / T_s$.

From equation (7), it can be known that the information from the vision system at step k represents the measurement at step k-n_{d_i}. It should be noticed that n_{d_i} is not constant due to the change of image processing time. In this research, T_{d_i} is assumed to be less than one sampling period of the camera, therefore, n_{d_i} can only be one value from the set {1, 2, …, 33} at an arbitrary i. In case of constant and small time delay, augmentation of state vector can be effectively employed. However, it is calculation intensive and complex for the random delay with large multi-ratio as discussed in this study.

B. Multiple Sampling Rates

In the combined system model, two different measurement times are available: the updating time of yaw rate is short (defined as T_s), and the sampling period of camera is much longer (defined as T_l). The multi-rate ratio n is defined as T_l/T_s. Therefore, the selection of T_s and T_l for system discretization needs to be considered. If the system sampling time is set to T_l, data from the high-speed sensors have to be dropped during inter-samples of the slow-speed device. This is a straightforward solution for the multi-rate issue but obviously deteriorates the estimation performance. An alternative method is to set the system sampling time to T_s; then, all the information from the fast-rate sensors can be utilized. However, as expressed in equation (8), visual data are not always available at every time step. Therefore, the inter-sample residuals of the visual information must be addressed.

$$y_k = \begin{cases} [\gamma_k \quad \psi_k \quad y_{lk}]^T & if \quad k = \left[(i-1) \cdot T_l + T_{d\_i} \right] / T_s , \\ [\gamma_k \quad 0 \quad 0]^T & if \quad k \neq \left[(i-1) \cdot T_l + T_{d\_i} \right] / T_s . \end{cases} \tag{8}$$

IV. Kalman Filter Considering Multi-rate and Measurable Uneven Delayed Measurements

As aforementioned, with the combined system model, two issues need to be considered in the Kalman filter design, namely, measurable uneven delay issue and multi-rate issue. Aimed at solving the uneven and multi-rate sampling issues, a multi-rate Kalman filter with inter-samples estimation is designed. Moreover, the multi-rate Kalman filter takes more information from high-speed sensors and increases the updating rate of the estimator for high-performance control.

First, the system is discretized with the sampling time of the fastest device (T is set to 1 ms in this research). Next, the time and measurement updates need to be designed. For the time update, the multi-rate Kalman filter can be implemented in the same way as the single-rate one. The camera's sampling period is T_l -T_{d_i}+T_{d_i+1} and during the sampling intervals, no information from the vision system is available. Therefore, pseudo-corrections have to be implemented for the operation of the measurement update. For Kalman filter design, measurements are utilized for residuals calculation, therefore, the residuals will be considered instead of the measurements in the remainder of this paper.

A. Reconstruction of Sampling Sequence

As can be seen in Fig. 2, the out-of-sequence visual information is not straightforward for fusion with other sensor signals, and it is therefore desired to reconstruct the visual signals. Consider that the image data are sampled at $(i\text{-}1) \cdot T_l$, but are not available until time $(i\text{-}1) \cdot T_l + T_{d\_i}$, it is reasonable to assume that the samplings are taken at $(i\text{-}1) \cdot T_l + T_{d\_i}$ instead of $(i\text{-}1) \cdot T_l$. Thus, the delay is removed from the reconstructed sampling sequence. As the measurements at $(i\text{-}1) \cdot T_l + T_{d\_i}$ represent the information at $(i\text{-}1) \cdot T_l$, and corresponding modification of residual is necessary.

After the above re-arrangement, the delays are removed from the measurements. However, the visual updates are still uneven and the sampling time is much longer than that of the yaw rate. The problem of this study is then transformed into designing a multi-rate Kalman filter for a discrete system with random multi-rate ratio. Two points need to be considered in this case: 1) residual modification at every $(i\text{-}1) \cdot T_l + T_{d\_i}$ time; 2) residual estimation between every neighbouring visual samples.

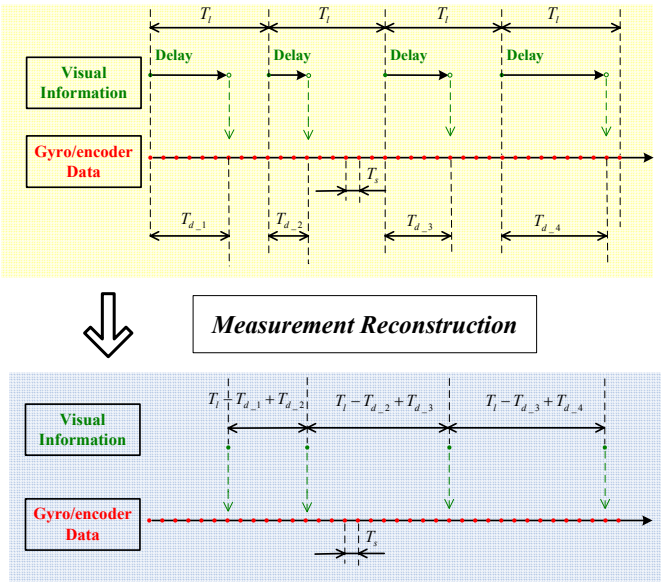

Fig. 3. Measurement reconstruction.

B. Residual Estimation Methodology

Remember that the vision model is free of uncertainty, i.e., the vision model can be trusted, it is possible to derive the propagation equations of the residual using the vision kinematic model. The definition of residual and estimation error are shown in equations (9) and (10), respectively. The two equations play important roles in the residual calculation.

$$\varepsilon_k^{vis} = y_k^{vis} - C \cdot \hat{x}_k^{vis-} \tag{9}$$

$$e_k^{vis} = x_k^{vis} - \hat{x}_k^{vis} \tag{10}$$

The overall algorithm can be summarized as: first consider the idea case when measurements are available at every T_s without delay, and derive the residual propagation equations. Then apply them to the multi-rate and delayed case.

In the idea case, from the definition of the estimation error, the estimation dynamics at step $k+j$ can be propagated using (11).

$$\begin{aligned} e_{k+j}^{vis} &= x_{k+j}^{vis} - \hat{x}_{k+j}^{vis} \\ &= x_{k+j}^{vis} - \hat{x}_{k+j}^{vis-} - K_{k+j}^{vis} \cdot (y_{k+j}^{vis} - C \cdot \hat{x}_{k+j}^{vis-}) \\ &= (x_{k+j}^{vis} - \hat{x}_{k+j}^{vis-}) - K_{k+j}^{vis} \cdot (C \cdot x_{k+j}^{vis} - C \cdot \hat{x}_{k+j}^{vis-}) \\ &= (I - K_{k+j}^{vis} \cdot C) \cdot G_{k+j-1}^{vis} \cdot e_{k+j-1}^{vis} \end{aligned} \tag{11}$$

The residual at step $k+j$ is given by equation (12), and it can be updated using equation (11).

$$\begin{aligned} \varepsilon_{k+j}^{vis} &= y_{k+j}^{vis} - C \cdot \hat{x}_{k+j}^{vis-} \\ &= C \cdot x_{k+j}^{vis} - C \cdot \hat{x}_{k+j}^{vis-} \\ &= C \cdot G_{k+j-1}^{vis} \cdot e_{k+j-1}^{vis} \end{aligned} \tag{12}$$

Combine equations (13) and (14) together, the propagation equation of residual is formulated as

$$\tilde{\varepsilon}_{k+j}^{vis} = \prod_{m=1}^{j} Q_{k+m} \cdot \varepsilon_k^{vis} \tag{13}$$

where

$$Q_m = C \cdot G_m \cdot (I - K_m \cdot C) \cdot C^T \left(C \cdot C^T \right)^{-1}$$

Then, apply the residual calculation equation to the reconstructed measurements. The algorithm can be generalized in three situations as follows:

1) Initial n_{d_1} steps:

   At step k in $[0, n_{d\_1})$, the residual ε_k is 0 due to the delay of measurement, i.e., the measurements are not available for initial residual calculation.

2) Reconstructed residual at each $(i\text{-}1)\cdot n + n_{d\_i}$ step:

   The measurement at each $(i\text{-}1)\cdot n + n_{d\_i}$ step represents information at step $(i\text{-}1)\cdot n$, and the correct residual at that step is given as

$$\varepsilon_{(i-1)\cdot n}^{vis} = y_{(i-1)\cdot n} - C \cdot x_{(i-1)\cdot n}^{vis-} \tag{14}$$

   Based on the propagation equation in (13), the residual at step $(i\text{-}1)\cdot n + n_{d\_i}$ can be calculated as

$$\varepsilon_{(i-1)\cdot n+n_{d\_i}}^{vis} = \prod_{m=1}^{n_{d\_i}} Q_{(i-1)\cdot n+m} \cdot \varepsilon_{(i-1)\cdot n}^{vis} \tag{15}$$

   This can be interpreted as: prepare the correct residual propagation matrix, and then calculate the final residual when measurements are available.

3) Inter-sample residual:

   The basic idea of the inter-sample residual estimation is to utilize the residual of the step 2) that is available and propagate it to the following inter-measurement steps. After $n\text{-}n_{d\_i\_1}+n_{d\_i}$ steps (delayed steps), the residual is recalculated when "new measurement" come in. However, it should be noticed that the so-called "new measurement" is not new because it is the delayed information. Between every two neighbouring

sampling times of the camera, the residual ε_k can be expressed as

$$\varepsilon_k^{vis} = \prod_{m=1}^{k-(i-1)\cdot n-n_{d\_i}} Q_{(i-1)\cdot n+n_{d\_i}+m} \cdot \varepsilon_{(i-1)\cdot n+n_{d\_i}}^{vis} \quad (16)$$

$$where \quad k \in \left((i-1)\cdot n+n_{d\_i},\ i\cdot n+n_{d\_i+1} \right)$$

V. Integrated Lateral Control for Electric Vehicles

As aforementioned, independent yaw control or lane keeping control has limitations. Therefore, controlling yaw motion and vehicle lateral position at the same time is desirable. As shown in Fig. 4, two controllers are incorporated in the system. The upper controller is designed for vehicle lateral position manipulation, i.e., if the vehicle is deviated from the desired path, the controller generates a steering control command for path correction. The lower controller is implemented for yaw motion stabilization based on the well-known two-degree-of-freedom controller and yaw moment observer (YMO) [1]. The steering input for vehicle position control generates a desired yaw rate (it is simplified as a first order transfer function in this simulation), and the differential torque of EVs can correct yaw motion in case of undesired vehicle movement. Obviously, there are two feedback loops: yaw rate feedback and lateral position feedback loops. Due to the sampling restriction of vision system, the two loops have different sampling rates. That is, yaw rate has higher sampling frequency than the visual information; moreover, the vision signals are contaminated by time-varying delays. Thus, the multi-rate Kalman filter considering measurable random delay proposed in the previous section can be employed to generate the lateral position signal at the same updating rate as yaw rate. Then, the sampling time of the overall system can be unified.

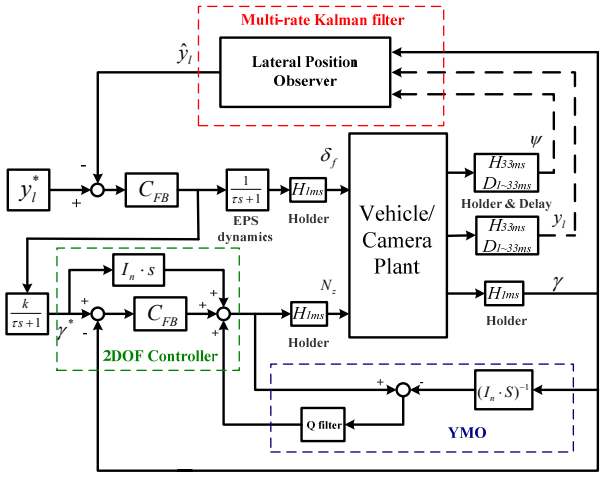

Fig. 4. Integrated lateral controller for EVs.

VI. Simulations and Experiments

A. Performance of the proposed multi-rate Kalman filter with random delay compensation

The performance of the proposed multi-rate Kalman filter was compared with the other methods in simulation. The vehicle was assumed to run at a speed of 25 km/h, and a sinusoidal steering input was given. To simulate real conditions, the vehicle model and the Kalman filter model were made different from each other. The random delay pattern was repeated as {20ms, 15ms, 10ms, 25ms}. The performance of the proposed method is shown in Fig. 5. For comparison, a method that assumes a constant delay is also provided. As can be observed, the measurement is random delayed and held; if a constant delay is assumed, the estimation performance is not satisfying. Meanwhile, the proposed multi-rate Kalman filter with measurement reconstruction and inter-sample compensation provided the best estimation result compared with the other methods. Field tests were conducted with our experimental vehicle. A sinusoidal steering input was provided by the driver, and the vehicle speed varied from 0 km/h to 30 km/h during the operation. Similar to the simulation settings, the C_f and C_r of the Kalman filter model were made different from those of the real vehicle. In fact, the true vehicle model can not be exactly known in all driving conditions. The proposed multi-rate Kalman filter with measurement reconstruction and residual compensation was compared with the constant delay method in Fig. 6. The multi-rate Kalman filter with constant delay compensation could not provide delay-free estimate as the proposed approach.

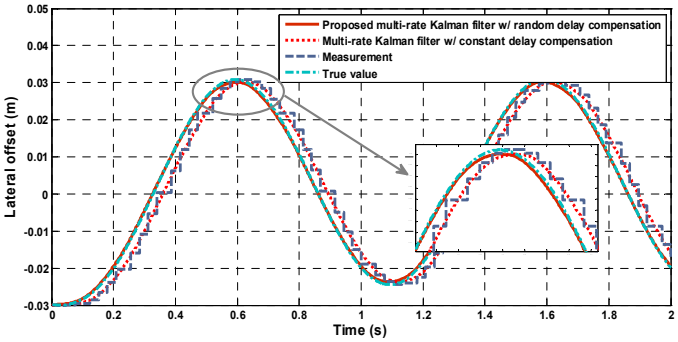

Fig. 5. Estimation methods comparison in simulation.

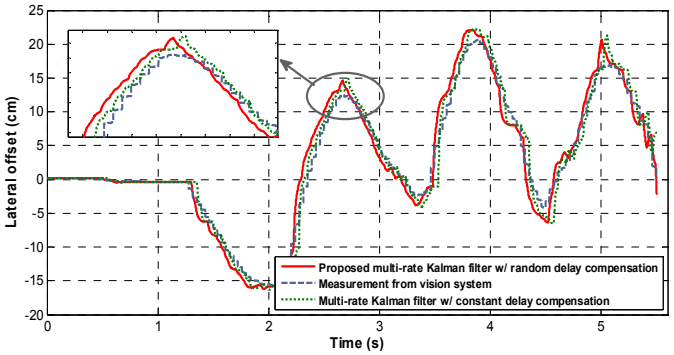

Fig. 6. Estimation methods comparison based on experimental data.

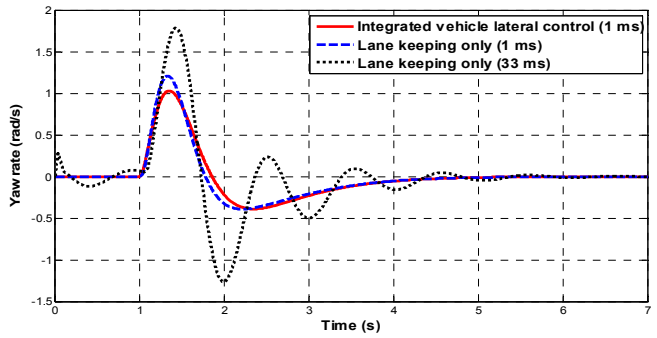

Fig. 7. Control performance comparison (yaw rate).

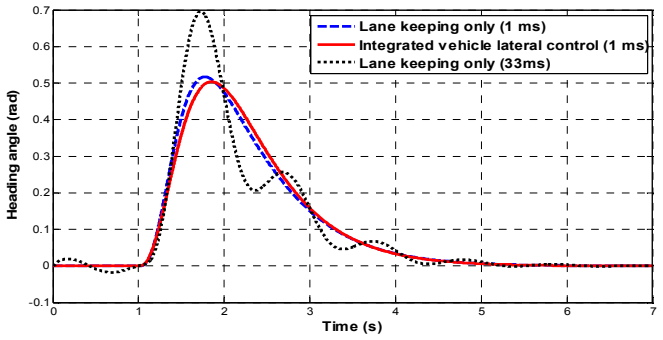

Fig. 8. Control performance comparison (heading angle).

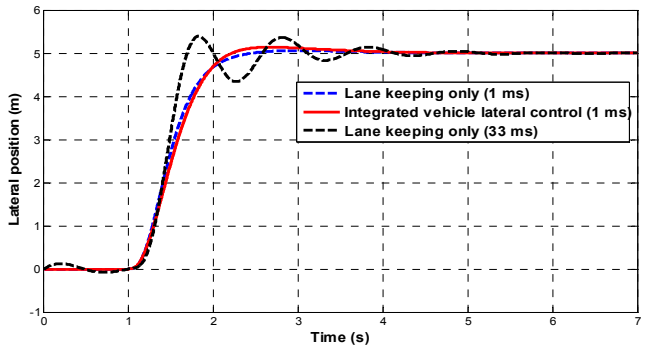

Fig. 9. Control performance comparison (lateral position).

B. Performance of the proposed controller

The proposed controller was verified by simulations, and traditional methods were also applied in the simulations for comparison. Fig. 7 shows the yaw rate control performance comparison. In case of lane keeping control only, the yaw rate in two traditional cases were very large. With the proposed integrated controller, yaw rate was suppressed effectively. Fig. 8 and Fig. 9 are the heading angle comparison and lateral position comparison, respectively. In case of position control only, yaw moment is zero, i.e., no control is applied, and a yaw moment is generated for the integrated vehicle lateral control. If a 33ms control period is assumed, both the heading angle and lateral position control performance were poor. In case of 1ms control period, the performances were improved, and the integrated controller can had the same performance as the 1ms lane keeping controller. In summary, if the vehicle is only controlled by a position controller, the yaw rate differs from the desired value and, the yaw rate in case of the integrated controller can make the vehicle track the desired value.

VII. CONCLUSIONS

In this paper, considering the importance of vehicle lateral control, a methodology for vehicle lateral position estimation was proposed. Then an integrated vehicle lateral controller to address both vehicle position and motion was developed. First of all, the combined vehicle and vision model was derived. Then, the multi-rate and measurable uneven time-delay issues were explained and formulated. Aimed at solving the uneven and multi-rate sampling issues, multi-rate Kalman filter is designed. Finally, simulation and experiment results were demonstrated to show the effectiveness of the proposed Kalman filter, and simulations were conducted to verify the integrated control system. The future work of this research is to apply the integrated controller to our experimental vehicle for realistic verification.

REFERENCES

[1] H. Fujimoto, N. Takahashi, A. Tsumasaka, T. Noguchi, “Motion control of electric vehicle based on cornering stiffness estimation with yaw-moment observer,” In proceeding of: Advanced Motion Control, 9th IEEE International Workshop on, 2006.

[2] Cong Geng, Lotfi Mostefai, Mouloud Denai and Yoichi Hori, “Direct Yaw Moment Control of an In-Wheel-Motored Electric Vehicle Based on Body Slip Angle Fuzzy Observer,” IEEE Transactions on Industrial Electronics, Vol.56, No.5, May 2009.

[3] J.C. McCall and M.M. Trivedi, “Video-based lane estimation and tracking for driver assistance: survey, system, and evaluation,” IEEE Trans. Intell. Transp. Syst., Vol. 7, pp. 20-37, 2006.

[4] M. Bertozzi and A. Broggi, “GOLD: A parallel real-time stereo vision system for generic obstacle and lane detection,” IEEE Trans. Image Process, Vol. 7, pp. 62-81, 1998.

[5] Byung-joo Kim, Huei Peng, “Vehicle Stability Control of Heading Angle and Lateral Deviation to Mitigate Secondary Collisions,” The 11th International Symposium on Advanced Vehicle Control, Seoul, Sept. 2012.

[6] Riccardo Marino, Stefano Scalzi, Mariana Netto, “Nested PID steering control for lane keeping in autonomous vehicles,” Control Engineering Practice, Volume 19, Issue 12, December 2011, Pages 1459-1467.

[7] Yafei Wang, Binh Minh Nguyen, Kotchapansompote, P., Fujimoto, H., Hori, Y., “Vision-based vehicle body slip angle estimation with multi-rate Kalman filter considering time delay,” Industrial Electronics (ISIE), 2012 IEEE International Symposium on, May 2012